THE JOURNAL OF BIOLOGICAL CHEMISTRY
Vol. 278, No. 27, Issue of July 4, pp. 24509–24520, 2003
Printed in U.S.A.

Detection of Conserved *N*-Linked Glycans and Phase-variable Lipooligosaccharides and Capsules from Campylobacter Cells by Mass Spectrometry and High Resolution Magic Angle Spinning NMR Spectroscopy*

Received for publication, February 5, 2003, and in revised form, April 25, 2003
Published, JBC Papers in Press, April 25, 2003, DOI 10.1074/jbc.M301273200

Christine M. Szymanski, Frank St. Michael, Harold C. Jarrell, Jianjun Li, Michel Gilbert, Suzon Larocque, Evgeny Vinogradov, and Jean-Robert Brisson‡

From the Institute for Biological Sciences, National Research Council of Canada, Ottawa, Ontario K1A 0R6, Canada

Glycomics, the study of microbial polysaccharides and genes responsible for their formation, requires the continuous development of rapid and sensitive methods for the identification of glycan structures. In this study, methods for the direct analysis of sugars from 10^8 to 10^{10} cells are outlined using the human gastrointestinal pathogen, *Campylobacter jejuni*. Using capillary-electrophoresis coupled with sensitive electrospray mass spectrometry, we demonstrate variability in the lipid A component of *C. jejuni* lipooligosaccharides (LOSs). In addition, these sensitive methods have permitted the detection of phase-variable LOS core structures that were not observed previously. High resolution magic angle spinning (HR-MAS) NMR was used to examine capsular polysaccharides directly from campylobacter cells and showed profiles similar to those observed for purified polysaccharides analyzed by solution NMR. This method also exhibited the feasibility of campylobacter serotyping, mutant verification, and preliminary sugar analysis. HR-MAS NMR examination of growth from individual colonies of *C. jejuni* NCTC11168 indicated that the capsular glycan modifications are also phase-variable. These variants show different staining patterns on deoxycholate-PAGE and reactivity with immune sera. One of the identified modifications was a novel –OP=O(NH_2)OMe phosphoramide, not observed previously in nature. In addition, HR-MAS NMR detected the *N*-linked glycan, GalNAc-α1,4-GalNAc-α1,4-[Glc-β1,3-]GalNAc-α1,4-GalNAc-α1,3-Bac, where Bac is 2,4-diacetamido-2,4,6-trideoxy-D-glucopyranose, in *C. jejuni* and *Campylobacter coli*. The presence of this common heptasaccharide in multiple campylobacter isolates demonstrates the conservation of the *N*-linked protein glycosylation pathway in this organism and describes the first report of HR-MAS NMR detection of *N*-linked glycans on glycoproteins from intact bacterial cells.

Carbohydrates are implicated in a variety of functions in all domains of life (1–6). There continues to be a growing demand for methodologies that can analyze carbohydrate structures with increasing levels of sensitivity and simplicity. Recent efforts by our laboratory to characterize the glycome of the important food-borne pathogen *Campylobacter jejuni* has led to the elucidation of all surface glycan structures (LOS,[1] CPS, and *N*-linked and *O*-linked glycans) and has provided us with an ideal system for the development and adaptation of rapid methods for glycan detection (7–11).

Genome sequencing of *C. jejuni* NCTC11168 demonstrated that the strain contained four gene clusters necessary for carbohydrate biosynthesis (12). The flagellar modification locus, adjacent to the flagellin structural genes *flaA* and *flaB*, encodes enzymes involved in the biosynthesis of *O*-linked pseudaminic acid and its derivatives (9). The LOS and adjacent protein glycosylation loci encode enzymes involved in the formation of outer core ganglioside mimics and bacillosamine-containing *N*-linked heptasaccharide, respectively (7, 8, 10, 11). Also, the capsular biosynthesis locus, containing a Kps transport system similar to that found in other encapsulated organisms, transfers a branched tetrasaccharide repeat to the outer membrane surface (7, 13, 14). The CPS product of this locus was subsequently demonstrated to be the major serodeterminant in the heat-stable typing scheme first described by Penner and Hennessy (14–16). However, an inconsistency in the literature developed when only a limited number of *C. jejuni* serotypes were believed to produce capsules based on detection by immunoblotting, yet all strains examined contained *kps* genes necessary for capsule transport. It was then shown in *C. jejuni* 81–176 that the high molecular weight CPS was antigenically variable, but it remained to be determined whether the loss in CPS reactivity was due to the lack of CPS production or changes in its structure (16).

Because capsular polysaccharides are the outermost structure on the bacterial cell, they play an important role in the interaction between the pathogen, host, and environment. In *C. jejuni* 81–176 the capsule is involved in INT407 cell inva-

* This work was funded by the National Research Council Genomics and Health Initiative. The costs of publication of this article were defrayed in part by the payment of page charges. This article must therefore be hereby marked "*advertisement*" in accordance with 18 U.S.C. Section 1734 solely to indicate this fact.

‡ To whom correspondence should be addressed: Institute for Biological Sciences, National Research Council of Canada, 100 Sussex Dr., Ottawa, Ontario K1A 0R6, Canada. Tel.: 613-990-3244; Fax: 613-941-1327; E-mail: jean-robert.brisson@nrc-cnrc.gc.ca.

[1] The abbreviations used are: LOS, lipooligosaccharide; Bac, bacillosamine, 2,4-diacetamido-2,4,6-trideoxy-D-glucopyranose; CE, capillary electrophoresis; CPMG, Carr-Purcell-Meiboom-Gill; CPS, capsular polysaccharide; DIPSI-2, decoupling in the presence of scalar interactions; ESI-MS, electrospray ionization mass spectrometry; GBS, Guillain-Barré Syndrome; HR-MAS, high resolution magic angle spinning; NOESY, nuclear Overhauser effect spectroscopy; TOCSY, total correlation spectroscopy; WURST-2, wideband, uniform rate, and smooth truncation; HMQC, heteronuclear multiple quantum correlation; HMBC, heteronuclear multiple bond correlation; *P*Etn, phosphorylethanolamine; *PP*Etn, pyrophosphorylethanolamine; GM1a, Galβ1,3GalNAcβ1,4[NeuAcα2,3]Galβ1,4Glc-ceramide; GD1a, NeuAcα2,3Galβ1,3GalNAcβ1,4[NeuAcα2,3]Galβ1,4Glc-ceramide.

sion, virulence in ferrets, serum resistance, and maintenance of bacterial cell surface hydrophilicity (16). Due to their variability and importance in pathogenesis, it is critical to be able to analyze these structures directly in their native state.

The *C. jejuni pgl* locus encodes enzymes necessary for the glycosylation of multiple proteins (17, 18), and disruption of this pathway by mutagenesis results in multiple pleiotropic effects (19). We recently identified many of the proteins modified by this pathway and determined the structure of the *N*-linked glycan to be GalNAc-α1,4-GalNAc-α1,4-[Glc-β1,3-]GalNAc-α1,4-GalNAc-α1,4-GalNAc-α1,3-Bac (8). However, it was currently unknown whether the same *N*-linked glycan is present in multiple campylobacter isolates or whether slight structural variations exist as is observed for the campylobacter *O*-linked flagellin glycan (9, 20).

C. jejuni LOSs have received much attention due to their unique mimicry of human ganglioside structures (21, 22) and their potential involvement in the induction of the autoimmune polyneuropathies, Guillain-Barré (GBS), and Miller Fisher syndromes (23, 24). *C. jejuni* LOSs have also recently been shown to be phase-variable and important in virulence (25–27). However, in the elucidation of *C. jejuni* LOS structures, there are two major problems, the need for a large amount of biomass and the time-consuming effort to isolate and purify LOSs.

Rapid and sensitive methods were thus developed for the analysis of campylobacter glycans to enable researchers to investigate these structures directly from the source and provide further clues about their roles in the multiple environments that this pathogen inhabits. Furthermore, these methods can also be adapted for the study of carbohydrates in other biological systems.

EXPERIMENTAL PROCEDURES

Bacterial Strains and Growth Conditions—*C. jejuni* NCTC11168 (HS:2) was isolated from a case of human enteritis (28) and later sequenced by Parkhill *et al.* (12). *C. jejuni* serostrains: HS:1 (ATCC 43429), HS:2 (ATCC 43430), HS:3 (ATCC 43431), HS:4 (ATCC 43432), HS:10 (ATCC 43438), HS:19 (ATCC 43446), HS:36 (ATCC 43456), and HS:41 (ATCC 43460) were obtained from ATCC; *C. jejuni* HS:23 was obtained from Dr. Peggy Godschalk, Erasmus University Medical Center, Rotterdam; *C. jejuni* OH4382 and OH4384 were obtained from Health Canada; and *Campylobacter coli* HS:30 (NCTC 12532) was obtained from NCTC. All campylobacter strains were routinely grown on Mueller Hinton agar (Difco) under microaerophilic conditions at 37 °C. *C. jejuni* NCTC11168 mutants were grown on Mueller Hinton agar with 30 μg/ml kanamycin.

Construction and Characterization of Site-specific Mutations—Construction of the *C. jejuni* NCTC11168 *kpsM* (7) and *pglB* (8) mutants has already been described.

Preparation of O-Deacylated LOSs from Cells for CE-MS Analysis—Overnight growth of *C. jejuni* from one agar plate ($\sim 10^{10}$ cells) was resuspended in phosphate-buffered saline, pH 7.4. The cells were pelleted (16,000 $\times$ *g* for 2 min) and then dehydrated in 70% ethanol followed by two washes with 95% ethanol and two washes of 100% acetone. The sample was then allowed to air-dry overnight. The dried cells were resuspended in 200 μl of deionized water containing 10 μg/ml proteinase K and incubated at 37 °C for 4 h. The temperature was raised to 75 °C for 10 min to stop the digestion, and the sample was lyophilized. The cells were then resuspended in 200 μl of 20 mM ammonium acetate buffer (pH 7.5) containing 100 μg/ml RNase and 50 μg/ml DNase and incubated at 37 °C for 6 h before being lyophilized. The digested cells were then stirred with 200 μl of hydrazine at 37 °C for 2 h to cleave the *O*-linked fatty acids of the LOS. The sample was placed in an ice bath, and the excess hydrazine was destroyed with cold acetone in dry ice. The deacylated LOS was isolated by centrifugation (16,000 $\times$ *g* for 15 min), and the product was washed again with acetone, centrifuged, resuspended in water, and centrifuged, and then the LOS-containing supernatant was lyophilized.

Spectroscopy—All CE-ESI-MS and CE-ESI-MS/MS experiments and structural analysis of the purified CPS by NMR were performed as previously described (7). ^{31}P NMR experiments were acquired using a Varian Inova 500-MHz spectrometer equipped with a *Z*-gradient 3-mm triple resonance (^{1}H, ^{13}C, and ^{31}P) probe as described before (29). External 85% phosphoric acid was used as the chemical shift reference.

Preparation of Cells for HR-MAS NMR—*C. jejuni* overnight growth from one agar plate ($\sim 10^{10}$ cells) was harvested and suspended in 1 ml of 10 mM potassium-buffered saline (pH 7) made in D_2O containing 10% sodium azide (w/v). The suspension was incubated for 1 h at room temperature to kill the bacteria. The cells were pelleted by centrifugation (7500 $\times$ *g* for 2 min) and washed once with 10 mM potassium-buffered saline in D_2O. The pellet was resuspended by adding 20 μl of D_2O, and then 40 μl of the suspension was inserted into the rotor for analysis.

HR-MAS NMR Spectroscopy—HR-MAS experiments were performed using a Varian Inova 600-MHz spectrometer equipped with a Varian nano-NMR probe as previously described (7, 8). Spectra from 40-μl samples were spun at 3 kHz and recorded at ambient temperature (21 °C). The experiments were performed with suppression of the HOD signal at 4.8 ppm. Proton spectra of bacterial cells were acquired with the Carr-Purcell-Meiboom-Gill (CPMG) pulse sequence (90-(τ-180-τ)$_n$-acquisition) (30) to remove broad lines arising from lipids and solid-like material. The total duration of the CPMG pulse (n*2τ) was 10 ms with τ set to (1/MAS spin rate). One-dimensional selective TOCSY experiments with various spin-lock times from 30 to 150 ms and selective NOESY with mixing times from 100 to 400 ms were performed as described previously (31, 32). For use under MAS conditions, the TOCSY sequences were modified so that the DIPSI-2 mixing sequence was replaced with the adiabatic WURST-2 pulses (8). Selective experiments were described as EXP(selected spins, selective excitation bandwidth, mixing time), where EXP is TOCSY or NOESY. Typically, proton spectra of bacterial cells could be obtained using 256–1024 transients (15 min to 1 h). For the selective experiments on the *N*-linked glycan resonances present as a minor component in the bacterial cells, the time for each TOCSY and NOESY varied from 1 to 8 h.

Deoxycholate-PAGE, Silver Staining, and Immunoblotting of Polysaccharides—Proteinase K-treated whole cells of *C. jejuni* wild type and phase variants were prepared and analyzed by deoxycholate-PAGE as previously described (7). One portion of the gel was silver-stained while the other portion of the gel was transferred to a polyvinylidene difluoride membrane (Roche Applied Science) and immunodetected with HS:2 antiserum (1:500 dilution). The immunoblot was then incubated with goat-anti-rabbit secondary antibody conjugated to alkaline phosphatase (1:2500 dilution, Sigma) and then developed with the nitro blue tetrazolium chloride/5-bromo-4-chloro-3-indolyl phosphate detection system (Roche Applied Science).

RESULTS

CE-MS Analysis of O-Deacylated C. jejuni NCTC11168 LOS—The use of *O*-deacylation to obtain MS with intact *C. jejuni* LOS has never been described in the elucidation of its structure. The adaptation of the method by Li *et al.* (33) allowed the quick screening of many strains and, when combined with serotyping and preliminary genetic knowledge, can provide a powerful tool in the prediction of LOS structures with as little as 10^8 cells. This method also permitted a glimpse at the deviating structure of the lipid A backbone, which was originally described by Moran *et al.* (34). *C. jejuni* is known to have both D-glucosamine (GlcN) and 2,3-diamino-2,3-dideoxy-D-glucose (GlcN3N) in the $\beta(1 \rightarrow 6)$-linked disaccharide lipid A backbone (Fig. 1*a*). As the method *O*-deacylation implies, only *O*-linked fatty acids are removed, thus allowing CE-MS observation of the additional *N*-linked fatty acids present in *C. jejuni*. Thus, the variability of the disaccharide backbone was observed firsthand in addition to the increased degree of phosphorylation (Fig. 1*a*) with phosphorylethanolamine (*P*Etn) yielding pyrophosphorylethanolamine (*PP*Etn). The CE-MS method also prevents the destruction of important constituents that are acid-sensitive, such as sialic acid, which tend to be lost during the mild acid hydrolysis routinely used to isolate the LOS core.

The first strain examined in this study was *C. jejuni* NCTC11168, whose complete LOS structure was recently reported by us (7). The *O*-deacylated LOSs of NCTC11168 yielded a variety of masses, where the major species was $[M-3H]^{3-}$ = 1184 (3555 Da; GlcN3N-GlcN backbone with *PP*Etn, Fig. 1*b*). Other variants shown in Table I include $[M-3H]^{3-}$ = 1108

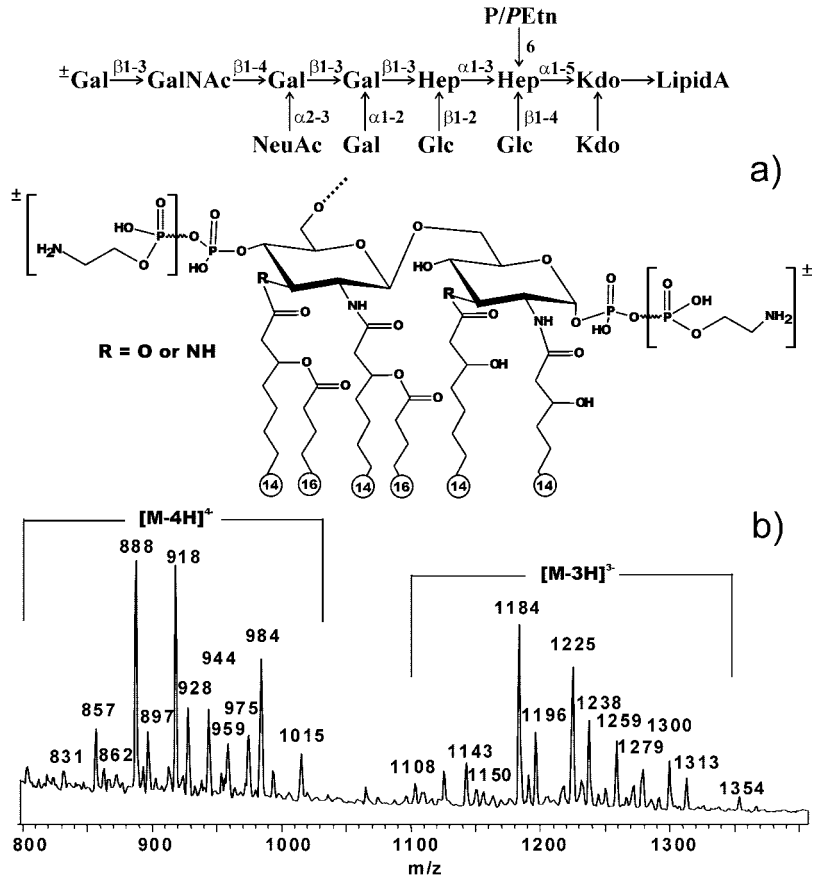

FIG. 1. **MS analysis of lipid A structure.** *a*, the chemical structure of the *C. jejuni* LOS and lipid A backbone. After *O*-deacylation, the *O*-linked fatty acids are lost, so that if either position labeled "*R*" is present as an amide (NH), the fatty acid remains adding 226 mass units to the observed mass. *b*, CE-MS analysis of *C. jejuni* NCTC11168 deacylated cells showing $[M\text{-}3H]^{3-}$ and $[M\text{-}4H]^{4-}$ mass ions.

TABLE I

Assignment of the variants for the lipid A backbones and variable terminal Gal of the deacylated LOS from C. jejuni NCTC11168

Assignments are from a comparison of the observed and calculated mass (Da) based on published LOS structures and lipid A structure (Fig. 1). The molecular masses of residues used: lipid A, 952; fatty acid (FA), 226; Neu5Ac; 291; HexNAc, 203; Glc/Gal, 162; Hep, 192; *P*Etn, 123; GalNAc, 203; and Kdo, 220.

Lipid A variant	t-Gal	Observed mass	Calculated mass
		Da	
GlcN-GlcN-*PP*Etn	−	3327	3326
GlcN-GlcN-2*PP*Etn	−	3453	3449
GlcN3N-GlcN	−	3432	3429
GlcN3N-GlcN-*PP*Etn	−	3555	3552
GlcN3N-GlcN	+	3591	3591
GlcN3N-GlcN-2*PP*Etn	−	3678	3675
GlcN3N-GlcN-*PP*Etn	+	3717	3714
GlcN3N-GlcN3N-*PP*Etn	−	3780	3778
GlcN3N-GlcN-2*PP*Etn	+	3840	3837
GlcN3N-GlcN3N-2*PP*Etn	−	3903	3901
GlcN3N-GlcN3N-*PP*Etn	+	3942	3940
GlcN3N-GlcN3N-2*PP*Etn	+	4065	4063

(3327 Da; typical di-GlcN backbone as seen in *Escherichia coli* but with *PP*Etn), $[M\text{-}3H]^{3-}$ = 1143 (3432 Da; GlcN3N-GlcN backbone), and $[M\text{-}3H]^{3-}$ = 1259 (3780 Da; GlcN3N-GlcN3N backbone with *PP*Etn). We are currently determining what conditions are responsible for the observed lipid A variation. The masses were further complicated by the fact that the terminal Gal is phase-variable (27) giving rise to masses of $[M\text{-}3H]^{3-}$ = 1196 (3591 Da), 1238 (3717 Da), and 1279 (3840 Da), to mention a few. To confirm the observation that the variability was either derived from the lipid A region or from the result of the phase-variable Gal, CE-MS/MS was used. From Fig. 2 (*a* and *b*) it can be seen that the MS/MS of $[M\text{-}3H]^{3-}$ = 1184 (3555 Da) and $[M\text{-}3H]^{3-}$ = 1225 (3678 Da) gave the same core mass of $[M\text{-}2H]^{2-}$ = 1015 (2031 Da; Kdo, 2Hep, *P*Etn, 2Glc, 3Gal, GalNAc, and Neu5Ac). Although the LOSs containing the extra Gal (Fig. 2*c*), $[M\text{-}3H]^{3-}$ = 1279 (3840 Da), gave a core mass of $[M\text{-}3H]^{3-}$ = 1096 (2194 Da; Kdo, 2Hep, *P*Etn, 2Glc, 4Gal, GalNAc, and Neu5Ac). CE-MS/MS also confirmed the presence of two Kdo residues in the core (data not shown). Therefore, when the alterations in lipid A and terminal Gal are overlooked, the core mass is consistent with the known structure. What is also interesting to note is that the core was always sialylated from growth to growth (results not shown), which is not always observed when the core is isolated through mild acid hydrolysis. However, changes in the ratio of GlcN *versus* GlcN3N and in the extent of phosphorylation were observed in the lipid A backbone and varied from growth to growth (results not shown) demonstrating that even the backbone is phase-variable and may perhaps play a role in virulence (35, 36).

CE-MS Analysis of LOSs from Other C. jejuni Strains—Other strains with known structures were also examined, including OH4382 and OH4384, HS:1, HS:2, HS:3, HS:4, HS:10, HS:19, HS:23, HS:36, and HS:41 (21). All strains showed a variable number of *N*-linked fatty acids, and many also showed increased phosphorylation of the lipid A region. However, most strains exhibited core masses consistent with their published structures when the lipid A variability was taken into account (Table II). The strains predominantly contained the GlcN3N-GlcN and GlcN3N-GlcN3N backbones and none of the GlcN-GlcN structure, with the exception of OH4382, which only displayed the GlcN3N-GlcN3N backbone. However, our studies also demonstrated some differences in the observed core structure in contrast to published studies (Fig. 3). *C. jejuni* HS:3 exhibited a terminal GalNAc residue that was always phosphorylated (only partially modified in the published structure) along with the potential of *P*Etn substitution at one of the

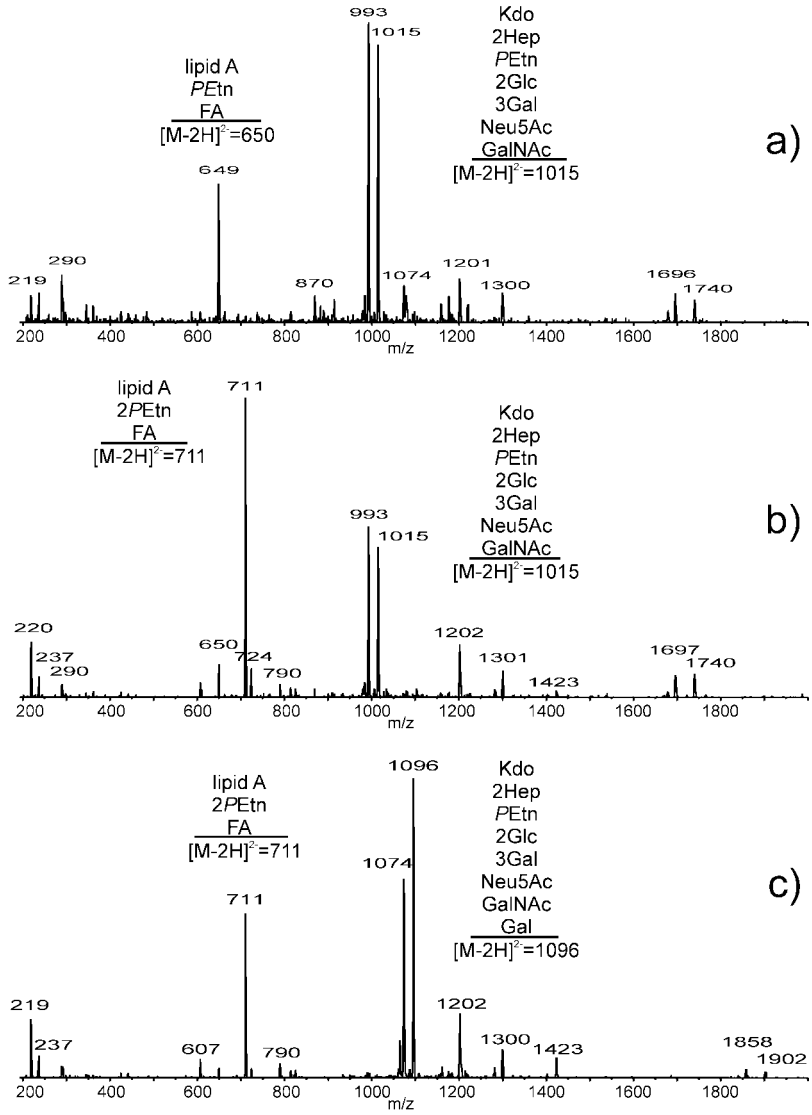

FIG. 2. **MS analysis of *C. jejuni* NCTC11168 *O*-deacylated cells.** CE-MS/MS of $[M-3H]^{3-}$ = 1184 (*a*), $[M-3H]^{3-}$ = 1225 (*b*), and $[M-3H]^{3-}$ = 1279 (*c*). *a versus b* shows that the lipid A portion differs by one *P*Etn ($[M-2H]^{2-}$ = 649 *versus* $[M-2H]^{2-}$ = 711), and *b versus c* shows the presence of the terminal Gal ($[M-2H]^{2-}$ = 1015 *versus* $[M-2H]^{2-}$ = 1096).

TABLE II

Assignment of the variants for the major lipid A backbones of the deacylated LOS from various strains of C. jejuni

Assignments are from a comparison of the observed and calculated mass (Da) based on published LOS structures as in Table I.

Strain	Lipid A variant mass											
	GlcN3N-GlcN		GlcN-GlcN3N-*PP*Etn		GlcN-GlcN3N-2*PP*Etn		GlcN3N-GlcN3N		GlcN3N-GlcN3N-*PP*Etn		GlcN3N-GlcN3N-2*PP*Etn	
	Obs.	Calc.	Obs.	Calc.	Obs.	Calc.	Obs.	Calc.	Obs.	Calc.	Obs.	Calc.
	Da											
HS:1	3432	3429	3555	3552	N/O[a]		3657	3655	3780	3778	N/O	
HS:2	3228	3226	3351[b]	3349	N/O		3453	3452	3576[b]	3575	N/O	
HS:3	N/O		3405	3403	N/O		N/O		3633	3629	N/O	
HS:4	3399	3396	3522	3519	3645	3642	3624	3622	3747	3745	3870	3868
HS:10	3561[b]	3558	3684	3681	3807	3804	3786	3784	3909	3907	4032	4030
HS:19	3399[b]	3396	3522	3519	3645	3642	3624[b]	3622	3747	3745	3870	3868
HS:23	N/O		2736	2734	2859	2857	N/O		2961	2960	3084	3083
HS:36	N/O		3231	3228	3354	3351	3333[b]	3331	3456	3454	3579	3577
HS:41	3108[b]	3105	3231	3228	3354	3351	3333	3331	3456	3454	3579	3577
OH4384	N/O		3813	3810	3936	3933	N/O		4038	4036	4161	4159
OH4382	N/O		N/O		N/O		3258	3257	3381	3380	3504	3503

[a] N/O, not observed.
[b] Trace amounts observed.

terminal or inner phosphate groups (not shown). The HS:10 serostrain only added *P*Etn as the phosphate substitution (37). *C. jejuni* HS:36 showed a variable terminal GalNAc, whereas HS:23 lacked the terminal Neu5Ac and GalNAc. In addition, cores of *C. jejuni* OH4382 (Fig. 4*a*) and HS:41 (Fig. 5*a*) exhibited an additional Neu5Ac residue compared with published reports.

CE-MS Analysis of LOS Sialylation—Due to the mildness of the method used, the extent of LOS sialylation could be observed in the samples analyzed. Strains that have one Neu5Ac

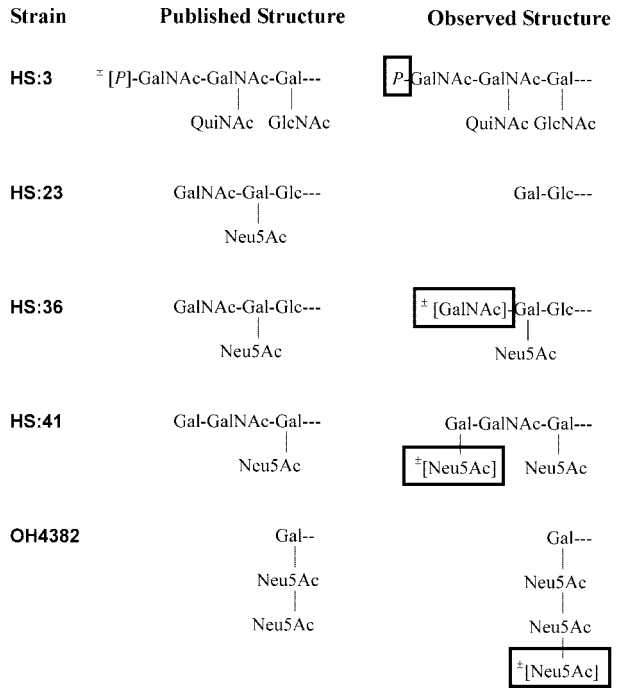

FIG. 3. **Differences between the published outer core LOS structures and the observed structures.** Additional and variable (±) modifications to the published structures are noted by *boxes* where as omissions are not indicated.

in their core (HS:1, HS:2, HS:23, and HS:36) were almost always sialylated (results not shown) with the exception of HS:23, which lacked Neu5Ac, possibly due to an inactive sialyltransferase (see "Discussion"). The strains with cores containing more than one Neu5Ac (OH4382, OH4384, HS:4, HS:10, HS:19, and HS:41) exhibited at least one Neu5Ac with the trend toward complete sialylation (>50%). Because some strains contained two Neu5Ac acids present as a chain, this was confirmed by CE-MS/MS by looking for the precursor ion at 581 Da (di-Neu5Ac). In HS:41, the second Neu5Ac was not attached to the first Neu5Ac, because a mass of 581 Da was not observed (Fig. 5*b*). As expected from the published structures, di-Neu5Ac chains were also not observed in HS:4 and HS:19 (21). The LOS of HS:10 was always sialylated, containing a terminal di-Neu5Ac chain, whereas the LOSs of OH4382 and OH4384 both contain up to three Neu5Ac residues. This is expected from the structure of OH4384 (21) and confirmed by the precursor ion at 581 Da. In the case of LOS from OH4382, the three Neu5Ac residues were present as a chain (Fig. 4*b*), because a precursor ion of 872 Da (tri-Neu5Ac) was observed.

Examination of CPS from Whole Cells by HR-MAS NMR—We recently described the capsular polysaccharide structure of the genome sequenced strain, NCTC11168 (HS:2) (7). The proton spectrum obtained from HR-MAS of suspended NCTC11168 bacterial cells closely resembled the spectrum of the purified capsular polysaccharide and clearly demonstrated the *N*-acetyl, *O*-methyl, and anomeric resonances (Fig. 6, *a* and *b*). Most significantly, the HR-MAS NMR spectrum was obtained in a few minutes directly from 40 μl of whole cells. Hence, this method permitted quick screening of campylobacter CPS directly from one plate of growth ($\sim 10^{10}$ cells) but was sensitive enough to detect a 1/100 dilution of the suspension containing 8×10^7 cells (Fig. 6*c*).

This method also permitted serotype comparisons between strains. The capsular polysaccharide structure from the HS:2 serostrain had not been determined. In fact, it was previously believed that this strain did not produce high molecular weight glycans and that seroreactivity was due to LOS (38). The CPS was not readily visible by Western blotting possibly due to the titer of sera used or the type of modification expressed (see analysis of NCTC11168 phase variants below). However, from microarray analysis it was shown that the HS:2 serostrain hybridized to all of the genes in the NCTC11168 capsule gene locus suggesting that both these strains produced similar structures (39). Consistent with the microarray findings, whole cell NMR spectra of the HS:2 serostrain and NCTC11168 are comparable (Fig. 6, *a* and *d*). These results provide further evidence that capsular polysaccharides are the main serodeterminant in the heat-stable typing scheme (14, 16) and demonstrate that HR-MAS NMR can be used to confirm serotype.

Although simple HR-MAS spectra of bacterial cells can allow one to monitor glycan resonances, assignment of resonances to specific residues may require further information. In the present study, selective TOCSY and NOESY experiments were employed to identify sugar residues or assign unknown resonances (32). For example, in the spectra of several campylobacter strains, sharp multiplets were often observed between 2.6 and 2.9 ppm (Fig. 6*d*). A series of selective TOCSY experiments identified all the spins for this compound, and they were determined to correspond to those of free aspartic acid. Addition of aspartic acid to the cells resulted in increased peak intensity between 2.6 and 2.9 ppm.

Also, selective TOCSY or NOESY could be performed on various *C. jejuni* serostrains to identify other sugar resonances in accordance with those reported in the literature. In the case of *C. jejuni* HS:41, previous studies have reported that the purified CPS was composed of a mixture of polysaccharides with the major and minor components differentiated by the presence of either 6-deoxyaltrofuranosyl or D-fucofuranosyl residues (40). The HR-MAS spectrum of HS:41 cells exhibited extensive spectral overlap so that signals for the signature 6-deoxy sugars could not be assigned unambiguously. However, selective TOCSY experiments on HS:41 cells (results not shown) starting with selective irradiation of ^{1}H resonances near 1.2 ppm established scalar coupling connectivities between the dominant CH_3 resonance at 1.27 ppm with other sugar ring protons whose chemical shifts (5.23, 4.25, 3.9, and 3.7 ppm) agreed with those of the 6-deoxy-D-altrofuranosyl moiety reported for the purified CPS (5.185, 4.19, 4.34, 3.71, and 3.89 ppm and CH_3 1.27 ppm) (40). These results suggests that the dominant form of the HS:41 CPS contains the 6-deoxyaltrofuranosyl moiety.

HR-MAS NMR Analysis of C. jejuni NCTC11168 CPS Phase Variants—While determining the structure of the major NCTC11168 CPS component, minor changes due to the addition and removal of certain groups were also observed (7), suggesting that a mixture of phenotypes existed in the population. To test this hypothesis, 10 single colonies of NCTC11168 were selected and restreaked to one plate each. The growth from a single plate was examined directly by HR-MAS NMR and also digested with proteinase K followed by deoxycholate-PAGE silver staining or immunoblotting. Three different phenotypes were observed by these methods. Growth from the first colony (variant 1) showed similar silver-staining patterns relative to the wild type population from which it was isolated from but showed increased levels of reactivity with HS:2 sera (Fig. 7, *a* and *b*). Comparison of the HR-MAS NMR spectra (Fig. 7) with those of the wild type NMR spectra of purified CPS (7) demonstrated that variant 1 predominantly exhibited a resonance at 3.2 ppm consistent with an *N*-ethanolamine modification on the glucuronic acid (Fig. 7*d*) in contrast to the major wild type form, which exhibited glucuronic acid modified with aminoglycerol (Fig. 7*c*). Variant 2 showed extremely reduced

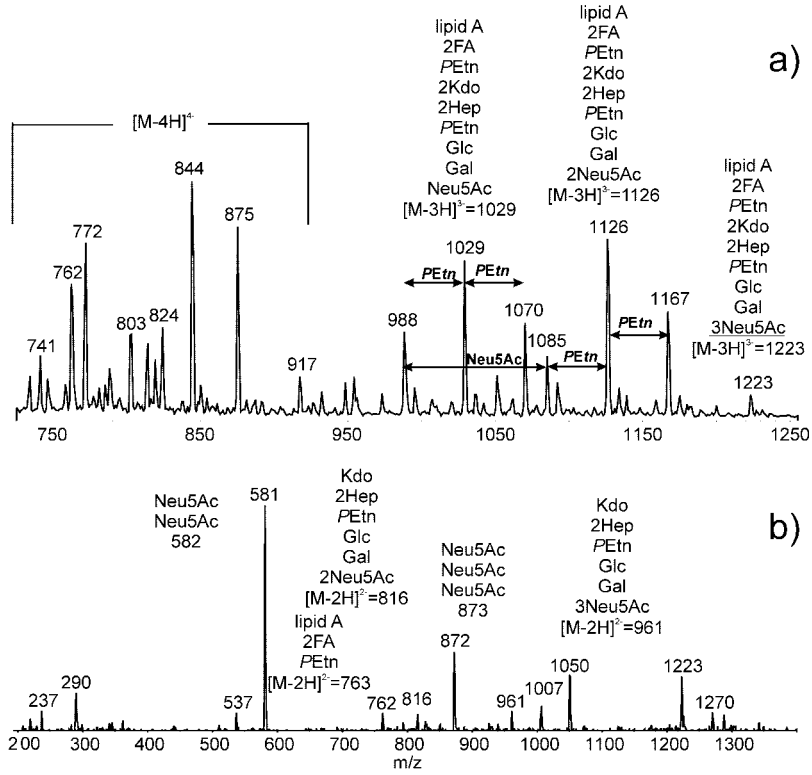

FIG. 4. **MS analysis of *C. jejuni* OH4382 *O*-deacylated cells.** *a*, CE-MS showing $[M-3H]^{3-}$ and $[M-4H]^{4-}$ mass ions. *b*, CE-MS/MS of $[M-3H]^{3-}$ = 1223 (which contains three Neu5Acs) showing that the Neu5Acs are present as a trimer (872 Da).

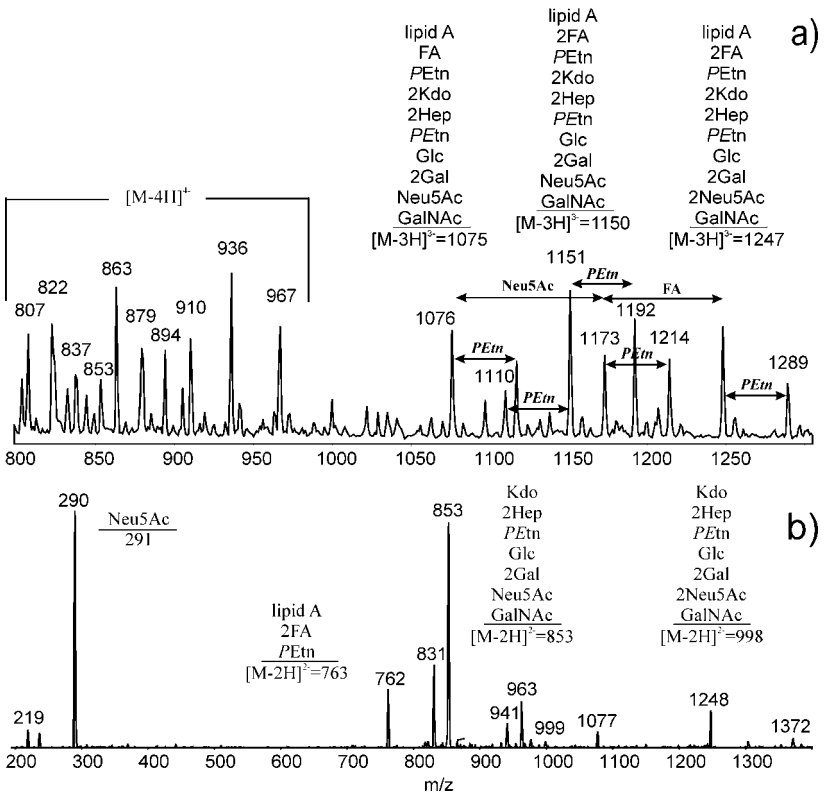

FIG. 5. **MS analysis of *C. jejuni* HS:41 *O*-deacylated cells.** *a*, CE-MS showing $[M-3H]^{3-}$ and $[M-4H]^{4-}$ mass ions. *b*, CE-MS/MS of $[M-3H]^{3-}$ = 1248 (which contains two Neu5Ac) showing that the Neu5Acs are present as monomers (290 Da) rather than as di-Neu5Ac units.

levels of silver staining and immunoblotting, although the HR-MAS spectra clearly indicated that similar amounts of polysaccharides were present in both variant and wild type samples (Fig. 7*e*). The HR-MAS spectrum of variant 2 revealed new resonances at 3.75 ppm (Fig. 7*e*) indicative of a novel modification, which had not been previously observed. In addition, the anomeric chemical shift for residue C moved downfield closer to the one for residue B. Variant 3 showed increased silver-staining but similar levels of immunoreactivity. This variant lacks the 6-*O*-Me group on the heptose confirmed by the loss of the resonance at 3.55 ppm (Fig. 7*f*).

The structural determination of the purified polysaccharide from *C. jejuni* NCTC11168 variant 2 was done as described before (7). Its backbone CPS structure was found to be the same as determined previously (Fig. 6) but with the addition of a modified phosphate group at C-3 of the Gal*f*NAc residue C (Fig.

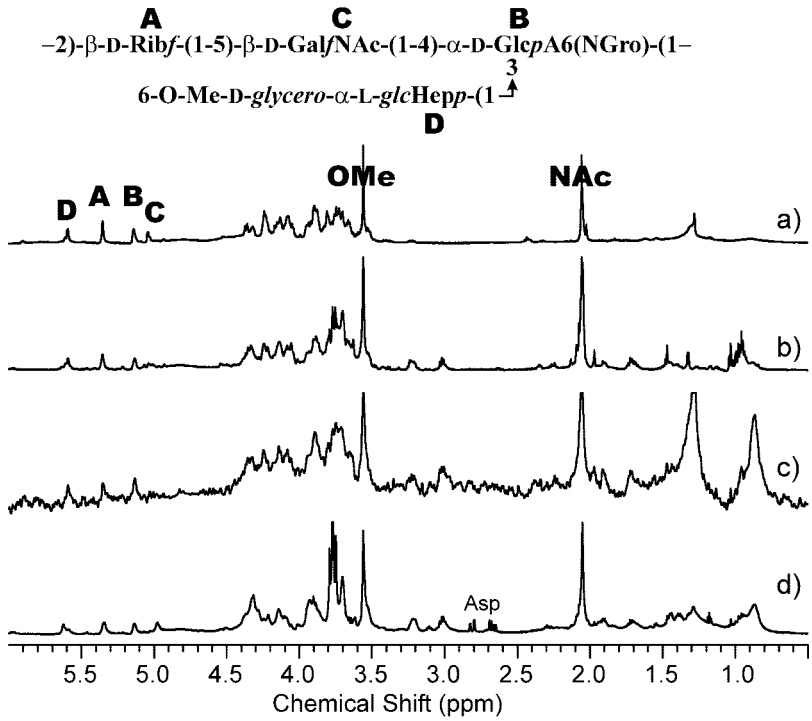

FIG. 6. **Proton NMR spectra of NCTC11168 and HS:2 serostrain.** *a*, ^{1}H spectrum of NCTC11168-purified CPS with the structure of the major component shown above. The anomeric, OMe, and NAc resonances are labeled. HR-MAS proton NMR spectra with a 10-ms CPMG filter of NCTC11168 whole cells (*b*), 1/100 dilution of whole cells (*c*), and HS:2 serostrain (*d*). The Asp (aspartic acid) resonances are labeled in *d*. The HOD resonance at 4.8 ppm was saturated and digitally filtered affecting the intensity of the anomeric resonance C in *b* and *c*.

8). The proton spectrum of the purified CPS from variant 2 is shown in Fig. 8*a*. The sample also contained about 30% of the major wild type CPS whose structure is shown in Fig. 6. Comparison of the HMQC spectra of variant 2 with the one from the wild type sample, showed similarity in chemical shifts for residues A, B, and D (Fig. 8*e* and Table III). Proton chemical shifts for residue C for variant 2 were identified using a selective TOCSY experiment (Fig. 8*b*). The 5D-4C and 3D-4C NOEs were also observed (Fig. 8*c*), as before for the wild type CPS (7).

The proton spectrum for variant 2 (Fig. 8*a*) contained a signal for the methyl group linked to phosphate via an ester bond: δ_H 3.75, δ_C 54.8 ppm, which had a $J_{P,H}$ of 11.5 Hz. In the ^{31}P-^{1}H HMQC spectrum (Fig. 8*d*) this methyl group showed correlation to the ^{31}P signal at 13.6 ppm, which also gave a correlation to H-3 of the Gal*f*NAc residue C. A $J_{P,H\text{-}3C}$ value of 8 Hz was obtained from simulation of the undecoupled ^{31}P spectrum. In the ^{31}P-^{1}H HMQC-TOCSY spectrum, correlations from the phosphorus signal at 13.6 ppm to H-2, H-3, H-4, and H-5 of the Gal*f*NAc residue were observed. These data indicated that the methyl phosphate group was linked at *O*-3 of the Gal*f*NAc residue C. However, the low field chemical shift of ^{31}P resonating at 13.6 ppm was inconsistent with the presence of a phosphodiester group.

In an attempt to isolate the phosphorylated monosaccharide, different conditions of mild acid hydrolysis of the polysaccharide were tested, in the hope that furanoside bonds could be cleaved without destruction of the phosphor-containing substituent. Hydrolysis with 1% trifluoroacetic acid for 20 min at 100 °C completely depolymerized the polysaccharide. At the same time the ^{31}P signal at 13.6 ppm disappeared, and a group of ^{31}P signals with one major component arose at ~2 ppm. All of them correlated with methyl group signals, with the major methyl signal observed at 3.88 (^{1}H)/56.7 (^{13}C) ppm. Milder hydrolysis conditions (1% trifluoroacetic acid at 60° or 2% AcOH at 100°, 1 h) led to incomplete conversion of the phosphate group but did not depolymerize the polysaccharide completely. Thus no method for the isolation of the modified monosaccharide in an intact form could be found. However, the chemical behavior and ^{31}P chemical shift of the methyl phosphate group were consistent with the presence of the amide of methylated phosphoric acid R–OP=O(NH_2)OMe. Phosphoramides can be hydrolyzed in dilute acids with the replacement of the NH_2 group with the OH group, in the conditions where alkyl esters of phosphoric acid are stable (41). Phosphoramides usually have ^{31}P signals between 10 and 20 ppm (42–48), which agrees with the position of the ^{31}P signal within the analyzed structure.

CE-MS Analysis of C. jejuni NCTC11168 CPS Phase Variant 2—To confirm the structure of the capsular glycan derived from NMR studies, the purified CPS sample was also analyzed by using CE-MS and CE-MS/MS techniques. All the CE-MS and CE-MS/MS experiments were acquired using high orifice voltage. With this experimental setup, the polysaccharide breaks up into shorter oligosaccharide units due to the front-end collision induced dissociation. In this study, an orifice voltage of 200 V was applied, and the extracted mass spectrum is shown in Fig. 9*a*. Compared with the spectrum obtained with a low orifice voltage (60 V), the typical polymer peak disappeared and strong peaks that correspond to oligosaccharide or monosaccharide units appear. The ion $[M + 1H]^+ = 884$ corresponded to the mass of the one repeat unit minus H_2O. The ion *m/z* 791 arose from the repeat unit of the wild type polysaccharide lacking unit E (30% of the sample) or the loss of unit E. The ions *m/z* 1181 and 1472 were assigned to one repeat unit plus CE, and to one repeat unit plus BD and A, respectively.

To further investigate the composition of the CPS repeat unit, the MS/MS experiments were conducted with the precursor ions at *m/z* 297, 382, 678, 884, 1181, and 1472. The MS/MS of ion *m/z* 297 clearly indicated the composition of C and E, whereas the MS/MS of ion *m/z* 382 displayed the composition of A and B (data not shown). Although the presence of the sugar residues D and A were not directly detected (Fig. 9*a*), the existence of these two residues in the oligosaccharide repeat unit from the tandem mass spectrum of ion *m/z* 884 could easily be determined. As shown Fig. 9*b*, there was a loss of 206 Da, which corresponded to the mass of residue D, resulting in the fragment ion *m/z* 678. Similarly, the fragment ions *m/z* 588, 456, and 429 were generated from the losses of CE (296 Da), AC (428 Da), and BD (455 Da), respectively. In Fig. 9*b*, the fragment ion at *m/z* 186 was assigned to the anhydrate C (203 Da)

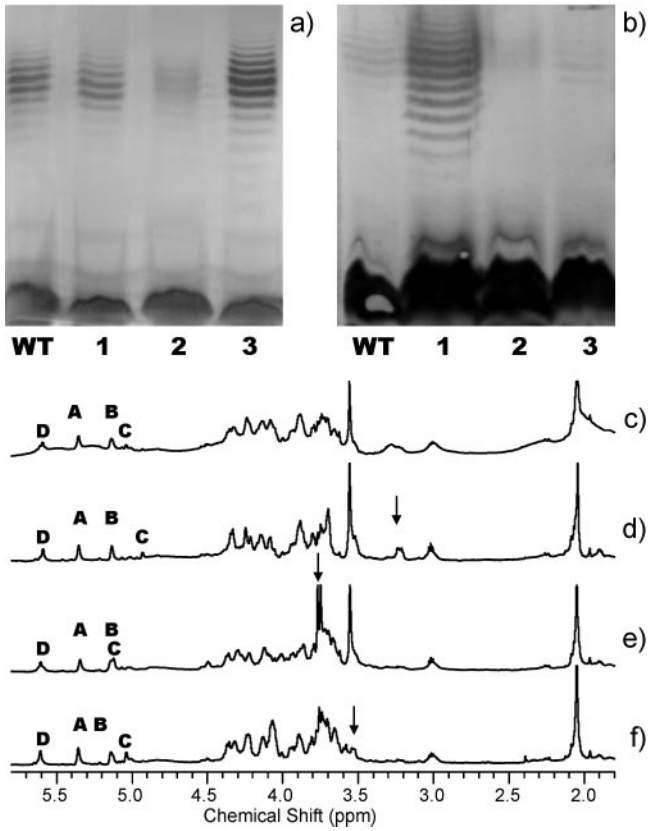

FIG. 7. **Comparison of individual colonies of NCTC11168.** *a*, silver-stained deoxycholate-PAGE: *lane 1*, NCTC11168 wild type population; *lane 2*, NCTC11168 variant #1; *lane 3*, NCTC11168 variant #2; *lane 4*, NCTC11168 variant #3. *b*, Western blot of the same samples loaded in the same order and immunodetected with HS:2 typing sera. HR-MAS NMR spectrum of the wild type population (*c*), variant #1 with arrow indicating presence of an ethanolamine resonance (*d*), variant #2 with arrow indicating presence of the novel modification (*e*), and variant #3 with the *arrow* indicating loss of OMe resonance (*f*). The anomeric resonances are labeled *A*, *B*, *C*, and *D*. Also note the movement of the anomeric peak for residue C in all variant spectra. The HOD resonance at 4.8 ppm was saturated and digitally filtered sometimes affecting the intensity of the anomeric resonance C.

and the ions at *m/z* 168 and 126 were generated from the consecutive neutral losses of H_2O (18 Da) and acetyl group (42 Da), respectively (29). The reason for the co-existence of fragment ions that correspond to losses of D, CE, ACE, and BD could be explained by the nature of generation of ions *m/z* 884, which is due to different breakage points along the polymer chain (A[CE][BD], [CE][BD]A, [BD]A[CE]). Hence, all the MS and MS/MS data were consistent with the structure for the CPS of variant 2 shown in Fig. 8.

Detection of N-Linked Glycans in Whole Cells by HR-MAS NMR—In the HR-MAS NMR spectra of intact campylobacter cells (Fig. 10), a set of common ^{1}H resonances was detected. We previously determined the structure of the *N*-linked glycan of *C. jejuni* NCTC11168 using MS and nano-NMR techniques to be a heptasaccharide (8). As can be observed in the HR-MAS spectra of *C. jejuni* NCTC11168, NCTC11168 *kpsM*-, *C. jejuni* HS:19, and *C. coli* HS:30, anomeric resonances, which matched those of the purified *N*-linked glycan, were observed, suggesting that this glycan was common to all (Fig. 10). In the spectra of NCTC11168 (Fig. 10*b*), resonances corresponding to the *N*-linked glycan were less intense than the resonances from the CPS, and some of the anomeric resonances overlapped. However, they could clearly be distinguished when the capsular resonances were eliminated in the NCTC11168 *kpsM* mutant (Fig. 10*c*). The assignment of the common glycan resonances to the *N*-linked glycan could be validated further by examining the spectra of the NCTC11168 *pglB* mutant in which protein glycosylation has been abolished (8, 17). As expected, the resonances of the *N*-linked glycan could not be observed in the NMR spectrum of this mutant (Fig. 10*f*).

The identity of the putative common glycan was further confirmed using selective TOCSY and NOESY experiments (Fig. 11). Experiments were carried out using *C. jejuni* HS:19 cells, because anomeric resonances of the *N*-linked glycan could be clearly observed. A standard selective NOESY experiment starting with selective irradiation of the **a1** resonance in HS:19 established a correlation with a resonance at 4.21 ppm (Fig. 11*a*). This resonance has the same chemical shift as the **a2** resonance observed in the NOESY spectra for the **a1** resonance in the purified glycopeptide (Fig. 11*b*). Comparison of the NOE patterns for other anomeric resonances between HS:19 and the purified *N*-linked glycan clearly indicated a similar match between the two sets of experiments (Fig. 11, *c–f*). Because the NOE experiments reveal both intra- and interresidue correlations, this agreement suggests that the sequence of the common glycan is identical to that of the purified *N*-linked glycan reported previously (8). A selective TOCSY experiment with irradiation of the **g1** and **f2** overlapping resonances at 4.5 ppm gave rise to cross-peaks corresponding to the **g2** and **f3** resonances (Fig. 11*g*). Their multiplet shape and chemical shifts matched those observed in the corresponding experiment for the purified *N*-linked glycan (Fig. 11*h*). Other resonances observed were due to partial excitation of the stronger CPS resonances. Hence, the selective excitation experiments performed on the bacterial cells established the *in situ* identity of the common *N*-linked glycan.

DISCUSSION

In this study, CE-MS/MS and HR-MAS NMR have been used successfully to examine glycan structures from 10^8 to 10^{10} bacterial cells. These methods can now be applied to investigate expression of glycans under different laboratory growth conditions and directly from the natural environments in which the pathogen is found. Examination of mutants will allow the assignment of genes involved in the biosynthetic pathways of these glycans and their modifications and help to determine the importance of structural phase variability in survival and pathogenesis. Due to the sensitivity and mildness of these methods, minor glycan structures that were not previously identified in the literature can also be detected.

The CE-MS/MS methods are particularly well suited to study variability in the LOS structures. The observed core replacement of phosphate with *P*Etn was not surprising, because this has been seen before in other *C. jejuni* strains (21). However, the cause of this variation still remains unknown. The absence/presence of the terminal GalNAc in the HS:36 serostrain is probably due to the presence of a phase-variable homopolymeric G-tract in *cgtA*, encoding the β-1,4-GalNAc transferase (10, 26), whereas the absence of the terminal GalNAc and Neu5Ac in HS:23 is probably due to the presence of the "phased-off" homopolymeric G-tract in *cstII* (sialyltransferase) (10). The terminal GalNAc in HS:23 would then not be added, because the GalNAc transferase needs a sialylated acceptor as was observed for the corresponding enzyme in HS:36 (10).

Our MS methods have also been useful for the examination of lipid A structure. Changes in the glucosamine backbone and in phosphorylation of the lipid A structure could easily be detected. Due to hydrazinolysis in our method, *O*-linked fatty acids are removed prior to MS analysis, but *N*-linked fatty acids can be observed. Micromethods to examine total fatty acids of lipid A are currently under development. Possible variations in lipid A backbone and fatty acid length may have important

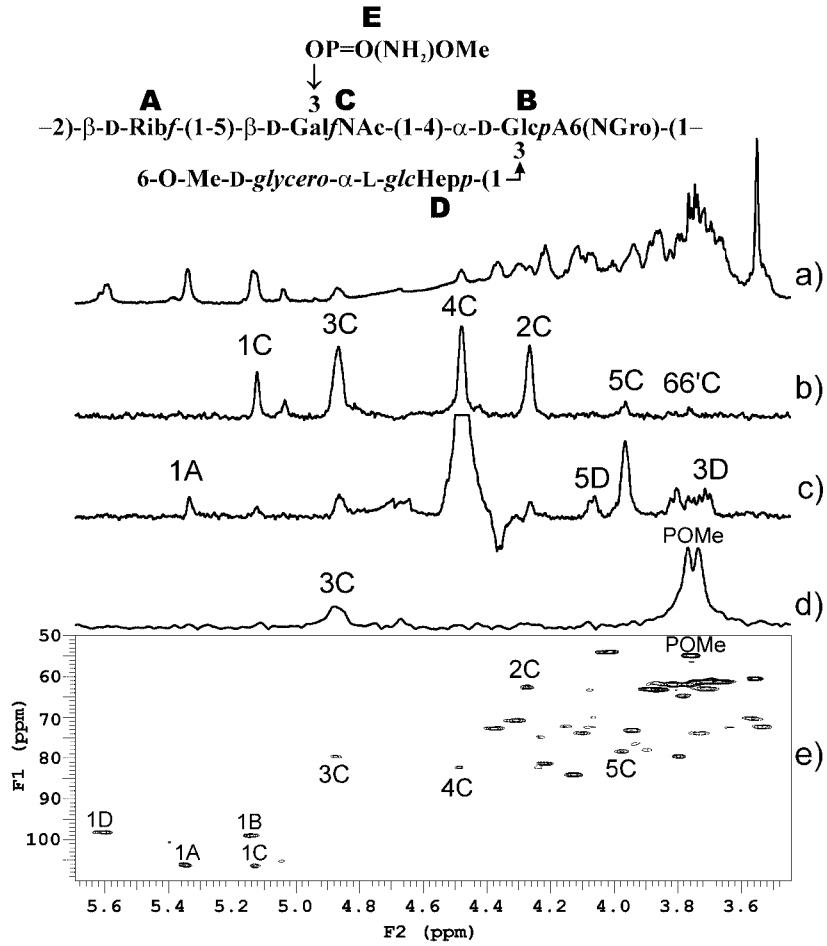

FIG. 8. **NMR experiments for the *C. jejuni* NCTC11168 variant 2 CPS.** The structure of the CPS is shown above the spectra. *a*, ^{1}H spectrum of the purified CPS. *b*, selective TOCSY (H-3C, 50 Hz, 80 ms) for assignments of the proton resonances of residue C. *c*, selective NOESY (H-4C, 50 Hz, 200 ms) to detect interresidue NOEs between residues C and D. *d*, trace from the ^{1}H-^{31}P HMQC for the ^{31}P signal at 13.6 ppm. *e*, ^{1}H-^{13}C HMQC spectrum showing assignments for residue C, the anomeric resonances, and the POMe (methyl phosphate) resonance.

TABLE III
Chemical shifts for the C. jejuni NCTC11168 variant 2 CPS

Shifts were measured at 600 mHz (^{1}H) in D_2O at 35 °C (±0.2 ppm error for δ_C and ±0.02 ppm for δ_H). Internal acetone CH_3 resonance was set at δ_H 2.225 ppm and δ_C 31.07 ppm.

Unit		1	2	3	4	5	6	7	8
						ppm			
A	δ_C	106.2	81.2	70.7	84.0	63.0			
	δ_H	5.35	4.21	4.30	4.13	3.89, 3.70			
B	δ_C	99.0	73.1	73.8	76.4	72.7	171.3[a]	53.9	61.3[b]
	δ_H	5.14	3.94	4.10	3.93	4.38	8.32[a]	4.03	3.72, 3.67[b]
C	δ_C	106.4	62.5	79.6	82.2	78.3	61.9	174.9[a]	22.9
	δ_H	5.13	4.27	4.88	4.48	3.97	3.82, 3.77	8.31[a]	2.05
D	δ_C	98.1	72.2	73.8	70.2	72.3	79.5	63.1	60.4
	δ_H	5.61	3.53	3.72	3.56	4.08	3.80	3.86	3.55
E	δ_C	54.8							
	δ_H	3.75							

[a] C=ONH: δ_C from HMBC at 25 °C; δ_H from ^{1}H spectrum in 90% H_2O/10% D_2O at 25 °C.
[b] $(CH_2)_2$ of glycerol (8B and 9B)

implications in eliciting host immune responses and in determining the extent of reaction against the LOS ganglioside mimics that have been suggested to play a role in GBS development. Indeed, variable acyl and *P*Etn groups have also been shown to be important for many bacteria in the development of immunity and bactericidal activity (35, 49), phase-variability (50), LOS regulation, and other functions (51). Interestingly, Bowes *et al.* (36) have recently shown that *C. jejuni* lipid A can cause B-cell-activated antiganglioside responses, but the portion of lipid A responsible for this activity has yet to be identified.

Accurate detection of sialylation for the prediction of ganglioside mimicry is important in trying to establish the correlation between campylobacter infection and GBS. We demonstrated that both the HS:41 serostrain and the GBS isolate, OH4382, have the ability to express additional Neu5Acs that were not observed previously. The observation of a third Neu5Ac in the LOS of OH4382 correlated with *in vitro* assays done with the OH4382 sialyltransferase enzyme, which can add a third sialic acid to a synthetic acceptor.[2] In HS:41, the additional sialic acid is suggested to be attached to the terminal Gal based on similar gene organization in the LOS biosynthetic locus of HS:41 compared with HS:4 and HS:19 (10). The ability of strains to produce multiple LOS structures provides further evidence for phase variation and expression of different gan-

[2] M. Gilbert, unpublished observation.

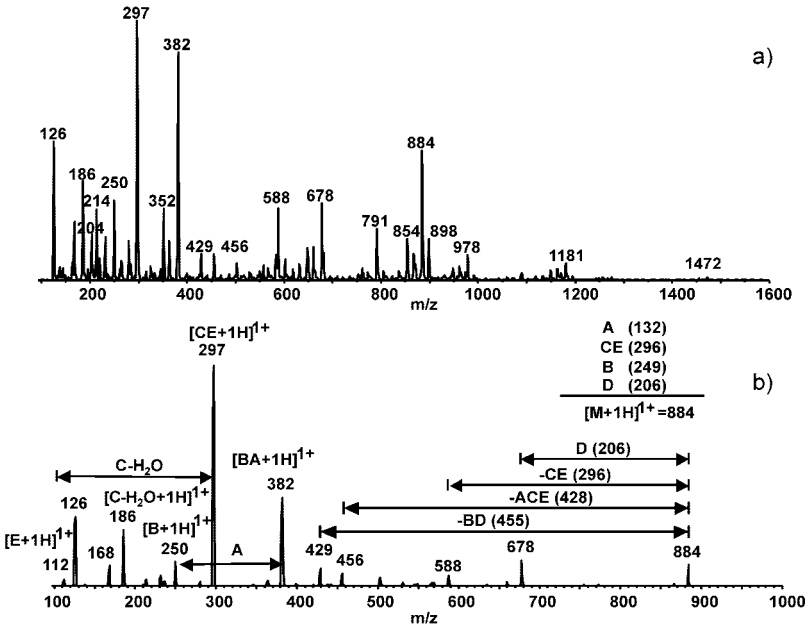

FIG. 9. **MS analysis for the *C. jejuni* NCTC11168 variant 2 CPS.** *a*, CE-MS (*m/z* 100–1600) with orifice voltage of 200 V. *b*, MS/MS spectrum of *m/z* 884 prompted by front-end collision-induced dissociation.

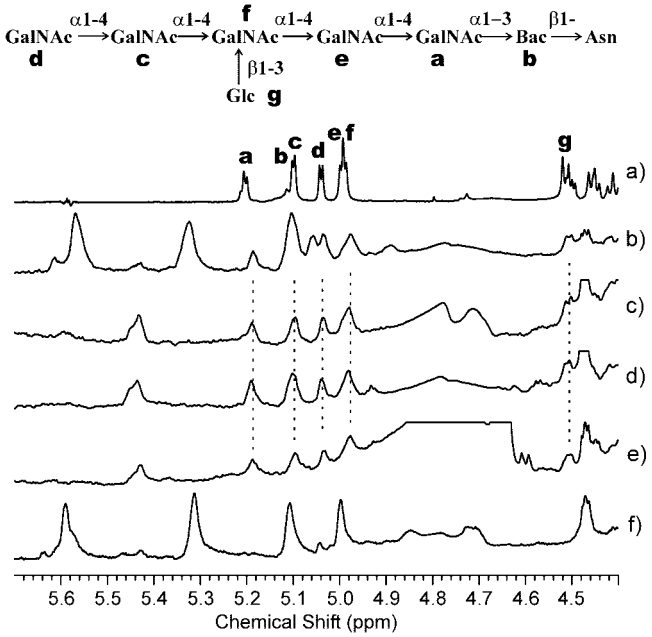

FIG. 10. **Detection of the *N*-linked glycan in the HR-MAS proton NMR spectra from various campylobacter strains.** The structure of the *N*-linked glycan is shown above the spectra. *a*, spectrum of the purified *N*-linked glycan in *C. jejuni* NCTC11168 showing the anomeric resonances labeled **a–g**. HR-MAS NMR spectra using a 10-ms CPMG filter of whole cells of *C. jejuni* NCTC11168 (*b*), *C. jejuni* NCTC11168 *kpsM*- (*c*), *C. jejuni* HS:19 serostrain (*d*), *C. coli* HS:30 serostrain (*e*), and *C. jejuni* NCTC11168 *pglB*- (*f*). Common resonances in *b–e* compared with those in *a* are indicated by *vertical dotted lines*. The HOD resonance at 4.8 ppm was saturated and digitally filtered.

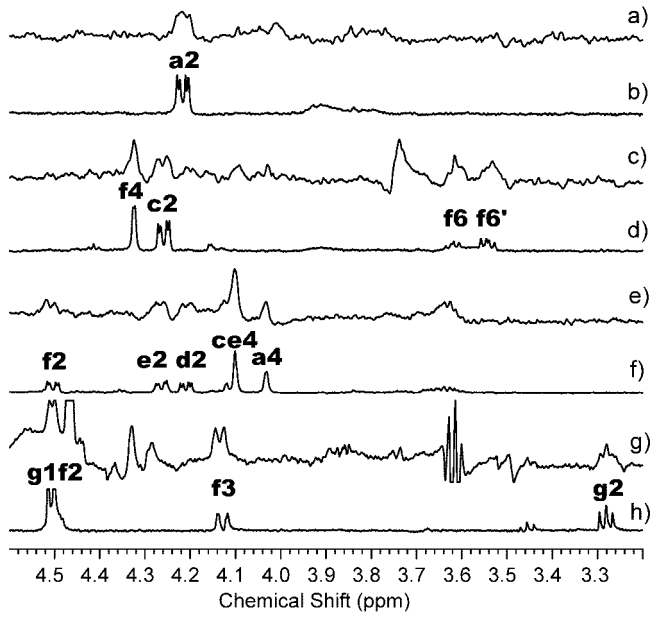

FIG. 11. **Comparison of selective NMR experiments of *C. jejuni* HS:19 cells and the purified *N*-linked glycan.** HR-MAS spectra of *C. jejuni* HS:19 (*a*, *c*, *e*, and *g*) and NMR spectra of the purified *N*-linked glycan (*b*, *d*, *f*, and *h*). *a*, NOESY (a1, 90 Hz, 250 ms); *b*, NOESY (a1, 40 Hz, 400 ms); *c*, NOESY (b1c1, 60 Hz, 250 ms); *d*, NOESY (b1c1, 40 Hz, 400 ms); *e*, NOESY (d1e1f1, 90 Hz, 250 ms); *f*, sum of NOESY (d1, 20 Hz, 400 ms) and of NOESY (e1f1, 25 Hz, 400 ms); *g*, TOCSY (g1f2, 72 Hz, 47 ms); and *h*, TOCSY (g1f2, 15 Hz, 33 ms).

glioside mimics in their LOS. Phase-variable ganglioside mimics were described previously (26, 27), and Guerry *et al.* (26) demonstrated that changes in the LOS structure affected invasion of tissue culture cells. Changes in sialylation can also affect LOS immunogenicity and serum sensitivity (25). It is interesting to note that both HS:19 and HS:41 serotypes have been associated with GBS (52), and this study demonstrates for the first time that HS:41 has the potential to produce the same GM1a/GD1a ganglioside mimics. Also, a correlation between the type of campylobacter ganglioside mimic present and the ensuing immune response and clinical outcome of the neuropathy has been shown (53). However, HS:4 is also reported to express the GM1a/GD1a structures, yet this serotype has not been linked with GBS induction. Bowes *et al.* (36) suggested that it is not only the ganglioside mimic that may be important in inducing an appropriate immune response but also the level of mimic expression. In addition, other factors such as the need to break down the host's immune tolerance are also involved, and this may be influenced by the potentially variable adjuvant activities of campylobacter lipid A. Therefore, the onset of GBS is multifactorial and probably dependent on both host and pathogen factors.

Recently, HR-MAS NMR has been used to detect the polysaccharides of lipopolysaccharide and CPS on intact bacteria (7,

54, 55). The method has also been used to detect nanomole amounts of purified lipopolysaccharide (54), purified *O*-linked and *N*-linked glycopeptides (8, 9, 56, 57), and LOS ganglioside mimics (11). In this study, HR-MAS NMR was used to further examine CPS directly from campylobacter cells. The CPS resonances could be readily identified and were in agreement with published spectra from purified CPS. In NCTC11168, the spectra clearly demonstrate the CPS anomeric protons from individual sugars and modifications, allowing simple screening of potential NCTC11168 capsular mutants to determine what residues are affected. Because capsular polysaccharides are the major serodeterminant of the heat-stable typing scheme, HR-MAS NMR also provides a quick method of determining whether strains belong to the same Penner serogroup.

HR-MAS NMR also allowed us to examine structural capsule variants from the diverse NCTC11168 population. Phase variability of campylobacter capsule structures was noted as early as 1991 by Mills *et al.* (58) when several strains showed serotyping differences after *in vitro* laboratory passage. The authors then observed differences in antibody response with typing sera after multiple *in vivo* samplings of the same strain (59). There is an abundance of variable bacterial sugar modifications mentioned in the literature, some of which have been recently summarized (7). A novel modification for *C. jejuni* NCTC11168 variant 2 was observed with –OP=O(NH_2)OMe on the 3-position of Gal*f*NAc. This structure, although present, could not be resolved in the previous study (7) due to its low abundance in the wild type population. Although the phosphoramide has not been described previously in nature, it shows structural similarity to synthetic organophosphate insecticides (60). Future studies will determine the relevance of these phase-variable modifications, identify the genes necessary for their biosynthesis, and examine the commonality of the phosphoramide addition.

The presence of aspartic acid in the HR-MAS spectra of many strains was also observed. This could be the result of excess aspartic acid from the media binding to whole cells or it could be an actual metabolite. We are currently investigating these possibilities. Interestingly, the presence of aspartic acid was not serostrain-dependent, because these resonances were present in the spectra of HS:2 cells but not in the spectra of NCTC11168 (HS:2). The fact that either the surface characteristics, causing media components to adhere differently, or the secreted metabolites vary in two strains that type as HS:2 is not surprising, because the biosynthetic genes encoding these serodeterminants are highly mobile, and therefore different genomes can acquire similar CPS loci by horizontal gene transfer (61).

In this study, we were able to determine the identity of the *N*-linked glycan in intact bacterial cells. Resonances from the *N*-linked glycan were seen in all *C. jejuni* strains examined and in *C. coli* HS:30. Previously, hybridization studies demonstrated that the *pgl* genes were present in *C. coli* HS:30 (17), and these genes have recently been identified in the genome sequence of *C. coli* HS:34 [3] demonstrating that this pathway and the bacillosamine-containing heptasaccharide are conserved in both human pathogens. For NCTC11168, the anomeric resonances for the *N*-linked glycan were buried under capsular anomeric resonances. However, in the acapsular *kpsM* mutant, the resonances could easily be identified. Also, as expected, resonances were not observed in the oligosaccharyltransferase mutant, *pglB*, providing further evidence that PglB enzyme inactivation results in inhibition of *N*-linked glycoprotein biosynthesis.

[3] C. Parker, personal communication.

It is generally accepted that a single microorganism can give rise to a diverse population with very different virulence properties. However, sensitive methods for the structural analysis of bacterial populations have been limiting. In this report, CE-MS/MS has been used to examine the structure and variability in *C. jejuni* LOS. HR-MAS NMR has been used to investigate CPS structure, confirm serotype, demonstrate population variability, study the effect of mutagenesis, and detect *N*-linked glycoprotein sugars. We have shown that campylobacter has a large repertoire of variable surface glycans in addition to a conserved *N*-linked glycan. These studies have implications in vaccine development, provide possibilities for the induction of GBS following campylobacter enteritis, describe methods that can be adapted for the analysis of glycans from other important bacterial pathogens, expand the new field of metabolomics, and can provide more insight into the importance of bacterial LOS, capsules, and protein glycosylation allowing scientists to expand the discipline of glycomics beyond the gene complement and glycan structure.

Acknowledgments—We thank Dr. Martin Young and Dr. Warren Wakarchuk for comments and support, Dr. Dennis Whitfield for helpful discussions, Health Canada for *C. jejuni* OH4382 and OH4384, Dr. Peggy Godschalk for *C. jejuni* HS:23, Nicolas Cadotte for technical support, Jeff Van Zetten for bacterial growth, and Dr. Kris Rahn for HS:2 antiserum.

REFERENCES

1. Dell, A., and Morris, H. R. (2001) *Science* **291,** 2351–2356
2. Hakomori, S. (2002) *Proc. Natl. Acad. Sci. U. S. A.* **99,** 10231–10233
3. Benz, I., and Schmidt, M. A. (2002) *Mol. Microbiol.* **45,** 267–276
4. Erridge, C., Bennett-Guerrero, E., and Poxton, I. R. (2002) *Microbes Infect.* **4,** 837–851
5. Rudd, P. M., Elliott, T., Cresswell, P., Wilson, I. A., and Dwek, R. A. (2001) *Science* **291,** 2370–2376
6. Krinos, C. M., Coyne, M. J., Weinacht, K. G., Tzianabos, A. O., Kasper, D. L., and Comstock, L. E. (2001) *Nature* **414,** 555–558
7. St. Michael, F., Szymanski, C. M., Li, J., Chan, K. H., Khieu, N. H., Larocque, S., Wakarchuk, W. W., Brisson, J. R., and Monteiro, M. A. (2002) *Eur. J. Biochem.* **269,** 5119–5136
8. Young, N. M., Brisson, J. R., Kelly, J., Watson, D. C., Tessier, L., Lanthier, P. H., Jarrell, H. C., Cadotte, N., St. Michael, F., Aberg, E., and Szymanski, C. M. (2002) *J. Biol. Chem.* **277,** 42530–42539
9. Thibault, P., Logan, S. M., Kelly, J. F., Brisson, J. R., Ewing, C. P., Trust, T. J., and Guerry, P. (2001) *J. Biol. Chem.* **276,** 34862–34870
10. Gilbert, M., Karwaski, M. F., Bernatchez, S., Young, N. M., Taboada, E., Michniewicz, J., Cunningham, A. M., and Wakarchuk, W. W. (2002) *J. Biol. Chem.* **277,** 327–337
11. Gilbert, M., Brisson, J. R., Kawarski, M. F., Michniewicz, J., Cunningham, A. M., Wu, Y., Young, N. M., and Wakarchuk, W. W. (2000) *J. Biol. Chem.* **275,** 3896–3906
12. Parkhill, J., Wren, B. W., Mungall, K., Ketley, J. M., Churcher, C., Basham, D., Chillingworth, T., Davies, R. M., Feltwell, T., Holroyd, S., Jagels, K., Karlyshev, A. V., Moule, S., Pallen, M. J., Penn, C. W., Quail, M. A., Rajandream, M. A., Rutherford, K. M., van Vliet, A. H., Whitehead, S., and Barrell, B. G. (2000) *Nature* **403,** 665–668
13. Whitfield, C., and Roberts, I. S. (1999) *Mol. Microbiol.* **31,** 1307–1319
14. Karlyshev, A. V., Linton, D., Gregson, N. A., Lastovica, A. J., and Wren, B. W. (2000) *Mol. Microbiol.* **35,** 529–541
15. Penner, J. L., and Hennessy, J. N. (1980) *J. Clin. Microbiol.* **12,** 732–737
16. Bacon, D. J., Szymanski, C. M., Burr, D. H., Silver, R. P., Alm, R. A., and Guerry, P. (2001) *Mol. Microbiol.* **40,** 769–777
17. Szymanski, C. M., Yao, R., Ewing, C. P., Trust, T. J., and Guerry, P. (1999) *Mol. Microbiol.* **32,** 1022–1030
18. Linton, D., Allan, E., Karlyshev, A. V., Cronshaw, A. D., and Wren, B. W. (2002) *Mol. Microbiol.* **43,** 497–508
19. Szymanski, C. M., Burr, D. H., and Guerry, P. (2002) *Infect. Immun.* **70,** 2242–2244
20. Logan, S. M., Kelly, J. F., Thibault, P., Ewing, C. P., and Guerry, P. (2002) *Mol. Microbiol.* **46,** 587–597
21. Moran, A. P., Penner, J. L., and Aspinall, G. O. (2000) in *Campylobacter* (Nachamkin, I., and Blaser, M. J., eds) pp. 241–257, American Society for Microbiology, Washington, D. C.
22. Moran, A. P., and Prendergast, M. M. (2001) *J. Autoimmun.* **16,** 241–256
23. Yuki, N., Yoshino, H., Sato, S., and Miyatake, T. (1990) *Neurology* **40,** 1900–1902
24. Jacobs, B. C., Endtz, H., van der Meche, F. G., Hazenberg, M. P., Achtereekte, H. A., and van Doorn, P. A. (1995) *Ann. Neurol.* **37,** 260–264
25. Guerry, P., Ewing, C. P., Hickey, T. E., Prendergast, M. M., and Moran, A. P. (2000) *Infect. Immun.* **68,** 6656–6662
26. Guerry, P., Szymanski, C. M., Prendergast, M. M., Hickey, T. E., Ewing, C. P., Pattarini, D. L., and Moran, A. P. (2002) *Infect. Immun.* **70,** 787–793
27. Linton, D., Gilbert, M., Hitchen, P. G., Dell, A., Morris, H. R., Wakarchuk, W. W., Gregson, N. A., and Wren, B. W. (2000) *Mol. Microbiol.* **37,** 501–514

28. Ahmed, I. H., Manning, G., Wassenaar, T. M., Cawthraw, S., and Newell, D. G. (2002) *Microbiology* **148,** 1203–1212
29. Kneidinger, B., O'Riordan, K., Li, J., Brisson, J. R., Lee, J. C., and Lam, J. S. (2003) *J. Biol. Chem.* **278,** 3615–3627
30. Meiboom, S., and Gill, D. (1958) *Rev. Sci. Instrum.* **29,** 688–691
31. Uhrin, D., and Brisson, J. R. (2000) in *NMR in Microbiology: Theory and Applications* (Barbotin, J. N., and Portais, J. C., eds) pp. 165–210, Horizon Scientific Press, Wymondham, UK
32. Brisson, J. R., Sue, S. C., Wu, W. G., McManus, G., Nghia, P. T., and Uhrin, D. (2002) in *NMR Spectroscopy of Glycoconjugates* (Jimenez-Barbero, J., and Peters, T., eds) pp. 59–93, Wiley-VCH, Weinhem
33. Li, J., Thibault, P., Martin, A., Richards, J. C., Wakarchuk, W. W., and vander Wilp, W. (1998) *J. Chromatogr. A* **817,** 325–336
34. Moran, A. P., Zahringer, U., Seydel, U., Scholz, D., Stutz, P., and Rietschel, E. T. (1991) *Eur. J. Biochem.* **198,** 459–469
35. Ernst, R. K., Yi, E. C., Guo, L., Lim, K. B., Burns, J. L., Hackett, M., and Miller, S. I. (1999) *Science* **286,** 1561–1565
36. Bowes, T., Wagner, E. R., Boffey, J., Nicholl, D., Cochrane, L., Benboubetra, M., Conner, J., Furukawa, K., Furukawa, K., and Willison, H. J. (2002) *Infect. Immun.* **70,** 5008–5018
37. Shin, J. E., Ackloo, S., Mainkar, A. S., Monteiro, M. A., Pang, H., Penner, J. L., and Aspinall, G. O. (1997) *Carbohydr. Res.* **305,** 223–232
38. Moran, A. P., and Penner, J. L. (1999) *J. Appl. Microbiol.* **86,** 361–377
39. Dorrell, N., Mangan, J. A., Laing, K. G., Hinds, J., Linton, D., Al Ghusein, H., Barrell, B. G., Parkhill, J., Stoker, N. G., Karlyshev, A. V., Butcher, P. D., and Wren, B. W. (2001) *Genome. Res.* **11,** 1706–1715
40. Hanniffy, O. M., Shashkov, A. S., Moran, A. P., Prendergast, M. M., Senchenkova, S. N., Knirel, Y. A., and Savage, A. V. (1999) *Carbohydr. Res.* **319,** 124–132
41. Barton, D. H. R., and Ollis, W. D. (1979) *Comprehensive Organic Chemistry*, 2nd. Ed., p. 1270, Pergamon Press, Oxford
42. Breil, S., Martino, R., Gilard, V., Malet-Martino, M., and Niemeyer, U. (2001) *J. Pharm. Biomed. Anal.* **25,** 669–678
43. Gilard, V., Martino, R., Malet-Martino, M., Niemeyer, U., and Pohl, J. (1999) *J. Med. Chem.* **42,** 2542–2560
44. Joqueviel, C., Martino, R., Gilard, V., Malet-Martino, M., Canal, P., and Niemeyer, U. (1998) *Drug Metab. Dispos.* **26,** 418–428
45. Shulman-Roskes, E. M., Noe, D. A., Gamcsik, M. P., Marlow, A. L., Hilton, J., Hausheer, F. H., Colvin, O. M., and Ludeman, S. M. (1998) *J. Med. Chem.* **41,** 515–529
46. Gilard, V., Martino, R., Malet-Martino, M. C., Kutscher, B., Muller, A., Niemeyer, U., Pohl, J., and Polymeropoulos, E. E. (1994) *J. Med. Chem.* **37,** 3986–3993
47. Gilard, V., Malet-Martino, M. C., De Forni, M., Niemeyer, U., Ader, J. C., and Martino, R. (1993) *Cancer Chemother. Pharmacol.* **31,** 387–394
48. Martino, R., Crasnier, F., Chouini-Lalanne, N., Gilard, V., Niemeyer, U., De Forni, M., and Malet-Martino, M. C. (1992) *J. Pharmacol. Exp. Ther.* **260,** 1133–1144
49. Berry, D. S., Lynn, F., Lee, C. H., Frasch, C. E., and Bash, M. C. (2002) *Infect. Immun.* **70,** 3707–3713
50. Mackinnon, F. G., Cox, A. D., Plested, J. S., Tang, C. M., Makepeace, K., Coull, P. A., Wright, J. C., Chalmers, R., Hood, D. W., Richards, J. C., and Moxon, E. R. (2002) *Mol. Microbiol.* **43,** 931–943
51. Lee, N. G., Sunshine, M. G., Engstrom, J. J., Gibson, B. W., and Apicella, M. A. (1995) *J. Biol. Chem.* **270,** 27151–27159
52. Nachamkin, I., Allos, B. M., and Ho, T. (1998) *Clin. Microbiol. Rev.* **11,** 555–567
53. Ang, C. W., Laman, J. D., Willison, H. J., Wagner, E. R., Endtz, H. P., De Klerk, M. A., Tio-Gillen, A. P., Van den, B. N., Jacobs, B. C., and van Doorn, P. A. (2002) *Infect. Immun.* **70,** 1202–1208
54. Jachymek, W., Niedziela, T., Petersson, C., Lugowski, C., Czaja, J., and Kenne, L. (1999) *Biochemistry* **38,** 11788–11795
55. Czaja, J., Jachymek, W., Niedziela, T., Lugowski, C., Aldova, E., and Kenne, L. (2000) *Eur. J. Biochem.* **267,** 1672–1679
56. Manzi, A. E., Norgard-Sumnicht, K., Argade, S., Marth, J. D., van Halbeek, H., and Varki, A. (2000) *Glycobiology* **10,** 669–689
57. Gallego, R. G., Blanco, J. L., Thijssen-van Zuylen, C. W., Gotfredsen, C. H., Voshol, H., Duus, J. O., Schachner, M., and Vliegenthart, J. F. (2001) *J. Biol. Chem.* **276,** 30834–30844
58. Mills, S. D., Kurjanczyk, L. A., Shames, B., Hennessy, J. N., and Penner, J. L. (1991) *J. Med. Microbiol.* **35,** 168–173
59. Aspinall, G. O., McDonald, A. G., Raju, T. S., Pang, H., Mills, S. D., Kurjanczyk, L. A., and Penner, J. L. (1992) *J. Bacteriol.* **174,** 1324–1332
60. Kasagami, T., Miyamoto, T., and Yamamoto, I. (2002) *Pest. Manag. Sci.* **58,** 1107–1117
61. Dingle, K. E., Colles, F. M., Ure, R., Wagenaar, J. A., Duim, B., Bolton, F. J., Fox, A. J., Wareing, D. R., and Maiden, M. C. (2002) *Emerg. Infect. Dis.* **8,** 949–955

Detection of Conserved *N*-Linked Glycans and Phase-variable Lipooligosaccharides and Capsules from Campylobacter Cells by Mass Spectrometry and High Resolution Magic Angle Spinning NMR Spectroscopy

Christine M. Szymanski, Frank St. Michael, Harold C. Jarrell, Jianjun Li, Michel Gilbert, Suzon Larocque, Evgeny Vinogradov and Jean-Robert Brisson

J. Biol. Chem. 2003, 278:24509-24520.
doi: 10.1074/jbc.M301273200 originally published online April 25, 2003
